Long-term evolution of luminescent properties in CdI$_2$ crystals

I. Karbovnyk, I. Bolesta, I. Rovetskyi, V. Lesivtsiv, Ya. Shmygelsky, and S. Velgosh

Department of Electronics, Ivan Franko National University of Lviv
107 Tarnavskogo Str., Lviv 79017, Ukraine
E-mail: ivan_karbovnyck@yahoo.com

A.I. Popov

Institute of Solid State Physics, University of Latvia, 8 Kengaraga Str., Riga LV-1063, Latvia

Fresh and aged melt-grown or gas-phase grown CdI$_2$ crystals are studied by means of low-temperature photoluminescence spectroscopy. Noticeable transformations of emission spectra are observed after long-term aging. The formation of nanostructures containing cadmium oxide and cadmium hydroxide as well as the changes in local surrounding of iodine atoms and the possible growth of polytypic modifications of CdI$_2$ are taken into account when considering the diversity of optical spectra.

Introduction

Cadmium iodide crystals are the representatives of MX$_2$ halide family. A notable feature of MX$_2$ crystals is their layered structure formed by a hexagonal close packing of iodine atoms, while a half of octahedral interstices in the lattice are filled with cadmium atoms. The principal structural element of the lattice is a $[Cd^{2+}I_6^-]^{4-}$ octahedral complex formed by Cd^{2+} in an octahedral interstice [1–4]. Previous investigations of CdI$_2$ crystals have been performed both theoretically [5–8] and experimentally [9–15].

The interaction between cadmium atoms and iodine atoms (that are easily polarisable) leads to the formation of I–Cd–I triple layers with a strong ionic-covalent bonding within the individual layer. The bonding energy, as estimated from the Cd–I dissociation energy is about 2.2 eV. Adjacent triple layers are weakly bonded by Van der Waals (VdW) interaction, therefore there is a significant anisotropy of bonding Cd–I/I–I forces [16].

A weak bonding between the adjacent layers allows the shifts of a part of the crystal along (0001) base planes. This circumstance, consequently, creates a one-dimensional (along c axis) structural disordering due to stacking faults. Being repeated periodically, such disordering results in polytypic modifications.

One-dimensional disordering can be revealed in x-ray diffraction (XRD) patterns as diffusion bands around 10l reflexes (where l = 0, 1, …). Another type of CdI$_2$ structural deformation is connected with the appearance of vertical walls formed by dislocations that govern the block-like structure of the crystal. It was revealed, that XRD patterns of CdI$_2$ undergo changes over time because of the movement of edge and partial dislocations due to a low binding energy (0.02 eV) between the adjacent I–Cd–I layers.

Aging processes are known to affect the functionality of various devices such as functional elements based on ceramics [17–19], polymer hybrid structures [20] or scintillators [21]. It was shown [22–24] that nanostructures are formed on the surface of CdI$_2$ crystals in the process of their aging in air. The formation mechanisms of nanostructures involve several stages: inception, growth and interaction between individual structures. In Ref. 22 it is established that these nanostructures contain cadmium oxide and cadmium hydroxide. A similar effect was observed in the photoluminescence studies of porous silicon (PS) [25], where quantum dots and quantum wires are formed from PS nanocrystals due to surface oxidation.

Since optical properties are also determined by the structure, one should expect evolution of optical response of CdI$_2$ over a long period of time. It has to be noted that all

CdX₂, (X = Br, Cl, I) crystals strongly differ from alkali and alkaline earth halides, where self-trapped holes (so-called V_k), F centers and defect formation via exciton decay are well established [26].

This work aims to study the emission spectra of CdI₂ crystals in the process of long-term aging. The principal tool for this study is a low-temperature luminescence spectroscopy.

Experimental

Melt-grown cadmium iodide crystals were obtained by means of the Bridgman–Stockbarger technique from a raw material, which was previously purified by applying zone meting [27]. Thin single crystalline plates of gas-phase grown CdI₂ were formed in the upper part of the growth ampule.

The low-temperature luminescence measurements were performed at SUPERLUMI beamline (HASYLAB at DESY, Hamburg) using 4–20 eV synchrotron radiation from the DORIS storage ring for excitation [28]. This experimental set-up is a unique tool for investigations of different types of wide band gap materials [29–34]. Synchrotron radiation intensity was 10^{12} photons per second. BM50 monochromator operating in a spectral range from 1.3 to 6.2 eV was employed to disperse the light emitted from the sample. The emission was eventually detected by the SI-440-UV photomultiplier operating in a photon counting mode.

Nuclear quadrupole resonance (NQR) spectra of ^{127}I isotope were recorded with the IS-3 radiospectrometer between 10 and 20 MHz at liquid nitrogen temperature.

Results and discussion

Time evolution of the CdI₂ emission spectra at a long-term (several years) aging in air is shown in Fig. 1. Freshly grown crystals (a bottom plot in Fig. 1) show an intensive band peaked at 2.48 eV (501 nm, *G*-band) with a

weak component on the long-wavelength shoulder (2.25 eV, 551 nm, *Y*-band). This emission does not depend on the excitation wavelength and is related to the radiative recombination of self-trapped excitons in $[Cd^{2+}I_6^-]^{4-}$ molecular complexes [35,36].

Long-term aging significantly changes the emission spectra of CdI₂. Middle and top plots in Fig. 1 show CdI₂ emission spectra after 2-year and 4-year aging, respectively. One can observe the shift of *G*- and *Y*-bands towards long-wavelength region. In the middle plot, the *G*-band is peaked at 2.42 eV (514 nm) and *Y*-band shifts to 2.04 eV (609 nm). Furthermore, the intensities of these bands are redistributed.

In the freshly grown crystal *G*-band is a dominant one. However, in the process of aging in air the intensity of *G*-band becomes comparable to that of the *Y*-band (see middle and bottom plots). It has to be mentioned that similar changes were observed in the luminescence spectra of CdI₂ films after their annealing at $T = 420$ K: in addition to *G*-band, an intensive luminescence around 2.2 eV (565 nm) was detected [37].

Further aging of CdI₂ (top plot) leads to the appearance of a narrow band with the maximum at 1.87 eV (665 nm) as well as of a long-wavelength emission around 1.68 eV (740 nm). The transformation of CdI₂ photoluminescence spectra over time, as supported by atomic force microscopy results, may be connected with the creation of nanostructures on the crystal surface [4,22–24] and with the modification of the crystal structure: the annihilation of moving defects and the appearance of PbI₂ nanophases.

Let us discuss the possible nature of the 1.87 eV emission. A specific feature of this narrow band is its bandwidth of FWHM = 0.05 eV, which is dramatically different from the respective values for other bands (see Table 1). It is plausible to assume that this band is related to CdO and Cd(OH)₂ nanoinclusions.

Nanophases are characterized by discrete energy spectra. Some of energy levels may be localized within the band gap of CdI₂. Optical transitions between these levels can be responsible for the 1.87 eV (665 nm) luminescence. The fact that the band position does not depend on temperature speaks in favor of such model, since the spectrum of nanophases is to a large extent determined by their small size, which is not strongly affected by temperature. The band at 1.68 (740 nm) is related to uncontrolled lead impurity.
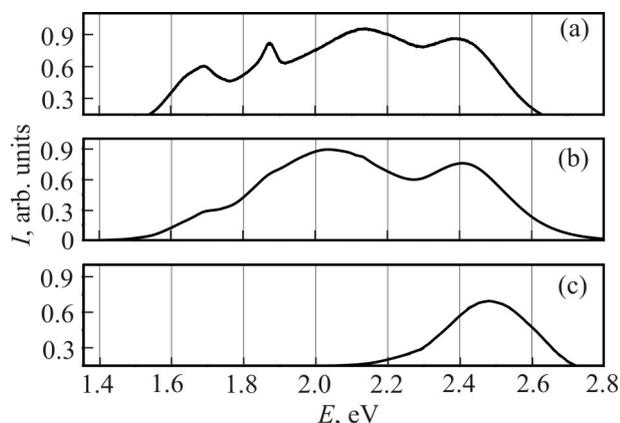

Fig. 1. Photoluminescence spectra of freshly melt-grown (c), 2-year aged (b) and 4-year (a) aged CdI₂ crystals. Spectra are recorded under the excitation by 12.4 eV (100 nm) photons at 8 K.

Table 1. Peak position and respective FWHM parameter for luminescence bands of aged melt-grown CdI₂ crystals

Energy, eV	FWHM, eV
1.68	0.08
1.87	0.05
2.13	0.18
2.44	0.09

We have also examined the changes in the emission spectra of aged melt-grown and gas-phase-grown CdI_2 crystals (see Fig. 2). In both spectra the band at 1.87 is clearly identified, whereas there are some noticeable differences in the short-wavelength region of the spectra.

One of the reasons for these differences is the crystal thickness: melt-grown samples are 0.1 to 0.5 mm thick, whereas the thickness of single-crystalline plates of gas-phase-grown CdI_2 does not exceed 10 μm. Thin crystals possess increased ratio of the number of surface atoms (N_s) to the number of bulk (N_v) atoms. Thus, surface atoms should have the prevailing contribution to the optical properties of the crystal. Geometrical order of atom distribution in the bulk (volume) and on the surface is also different. This conclusion is confirmed by nuclear quadrupole resonance (NQR) frequency studies of ^{127}I in CdI_2 crystals.

NQR measurements of ^{127}I in melt-grown CdI_2 crystals show two maxima at 14.34 and 4.74 MHz, while four NQR maxima at 14.07, 14.33, 14.74 and 15.02 MHz were observed in gas-phase-grown crystals (see Fig. 3).

Thus, the emission spectra for melt- or gas-phase-grown CdI_2 crystals should be different as well, since they are defined by both the electronic structure of centers and the local surrounding. Hence, the structure of $[Cd^{2+}I_6^-]^{4-}$ complexes localized in the volume (bulk) or on the surface is different.

Two pronounced maxima at $\nu_1 = 14.34$ MHz and $\nu_2 = 14.74$ MHz (exact frequencies may slightly vary from sample to sample) correspond to two unequal crystallographic positions of iodine in the unit cell of CdI_2. The other two maxima at $\nu' < \nu_1$ and $\nu'' > \nu_2$ may be related to surface iodine atoms that have a different crystallographic surrounding.

Another possible reason for the observed differences in optical spectra can be related to the emission from the nanophases formed on the CdI_2 surface. The contribution
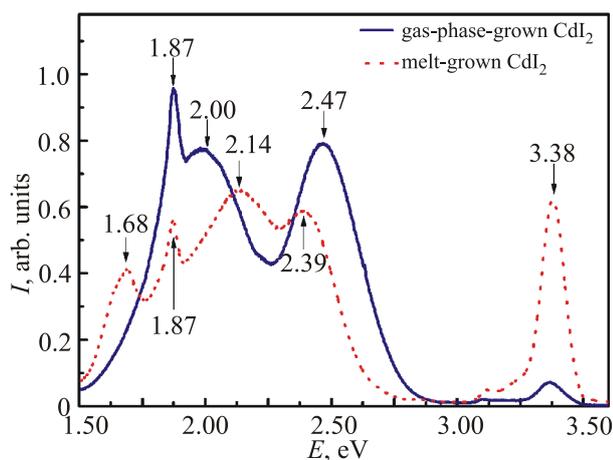

Fig. 3. NQR spectra of ^{127}I isotopes in melt-grown and gas-phase-grown CdI_2 crystals.

of these nanophases to the total luminescence yield should be larger in case of gas-phase-grown CdI_2, since due to a small thickness the concentration of centers inside nanophases is increased with respect to the concentration of intrinsic emission centers. The latter conclusion is confirmed by different intensities of intrinsic emission of CdI_2 in a spectral region about 3.38 eV (see Fig. 2).

At the same time, various polytypic modifications could be formed in gas-phase-grown CdI_2 crystals and their emission spectra are sensitive to the structure of a specific polytype.

It is very likely that all mentioned factors occur simultaneously, governing the complex time evolution of a low temperature photoluminescence in CdI_2.

Conclusions

Long-term aging of CdI_2 crystals leads to the modification of their low-temperature luminescence spectra. In the freshly grown crystals, green luminescence is prevailing, while upon aging in air, the intensity of yellow emission grows considerably. This fact can be associated with the formation of nanostructures on the crystal surface and their transformation over time. Different structure of $[Cd^{2+}I_6^-]^{4-}$ complexes localized in the bulk and on the surface determines the distinctions in the emission spectra of melt-grown and gas-phase-grown CdI_2 crystals.

Fig. 2. Luminescence spectra measured for melt-grown and gas-phase-grown CdI_2 crystals at the excitation by 12.4 eV photons at $T = 8$ K.

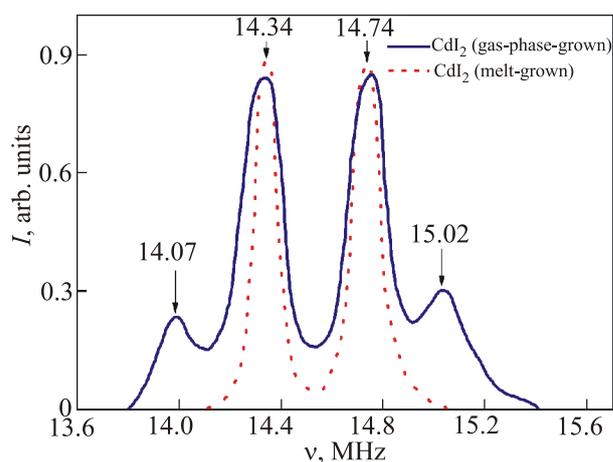1. R.M. Bozorth, *J. Am. Chem. Soc.* **44**, 2232 (1922).
2. I. Bolesta, S. Velgosh, Yu. Datsiuk, I. Karbovnyk, V. Lesivtsiv, T. Kulay, A.I. Popov, S. Bellucci, M. Cestelli Guidi, A. Marcelli, and M. Piccinini, *Radiat. Meas.* **42**, 851 (2007).

3. S. Bellucci, I. Bolesta, M. Cestelli Guidi, I. Karbovnyk, V. Lesivciv, F. Micciulla, R. Pastore, A.I. Popov, and S. Velgosh, *J. Phys.: Condens. Matter* **19**, 395015 (2007).

4. I. Karbovnyk, I. Bolesta, I. Rovetskii, S. Velgosh and H. Klym, *Mater. Science-Poland* **32**, 391 (2014).

5. R. Coehoorn, G.A. Sawatzky, C. Haas, and R.A. de Groot, *Phys. Rev. B* **31**, 6739 (1985).

6. J. Robertson, *J. Phys. C:* **12**, 4753 (1979).

7. M.G. Brik, I.V. Kityk, K. Ozga, and A. Slezak, *Physica B* **406**, 192 (2010).

8. Qi-Jun Liu, Zheng-Tang Liu, and Li-Ping Feng, *Phys. Status Solidi B* **248**, 1629 (2010).

9. I. Pollini, J. Thomas, R. Coehoorn, and C. Haas, *Phys. Rev. B* **33**, 5747 (1986).

10. C.R. Ronda, E. Zwaal, H.F. Folkersma, A. Lenselink, and C. Haas, *J. Solid State Chem.* **72**, 80 (1988).

11. S. Kondo, S. Matsuoka, and T. Saito, *Phys. Status Solidi A* **165**, 271 (1998).

12. M.I. Miah, *Opt. Commun.* **284**, 5199 (2011).

13. M.I. Miah, *Mat. Chem. Phys.* **119**, 402 (2010).

14. I.S. Yahia, M. Shapaan, Yasser A.M. Ismail, A.M. Aboraia, and E.R. Shaaban, *J. Alloys Compounds* **636**, 317 (2015).

15. I. Karbovnyk, V. Lesivciv, I. Bolesta, S. Velgosh, I. Rovetsky, V. Pankratov, C. Balasubramanian, and A.I. Popov, *Physica B* **413**, 12 (2013).

16. M.A. Wahab, *Solid State Commun.* **36**, 885 (1981).

17. H. Klym and A. Ingram, *J. Phys.: Confer. Ser.* **79**, 012014 (2007).

18. H. Klym, I. Hadzaman, O. Shpotyuk, Q. Fu, W. Luo, and J. Deng, *Solid State Phenom.* **200**, 156 (2013).

19. A. Bondarchuk, O. Shpotyuk, A. Glot, and H. Klym, *Rev. Mex. Fís.* **58**, 313 (2012).

20. I.B. Olenych, O.I. Aksimentyeva, L.S. Monastyrskii, and M.R. Pavlyk, *J. Appl. Spectrosc.* **79**, 495 (2012).

21. I.M. Bolesta, B.M. Kalivoshka, I.D. Karbovnyk, V.M. Lesivciv, I.S. Novosad, S.S. Novosad, I.M. Rovetskyy, and S.R. Velgosh, *Mater. Science-Poland* **32**, 604 (2014).

22. I.M. Bolesta, I.N. Rovetskyj, M.V. Partyka, I.D. Karbovnyk, and B.Ya. Kulyk, *Ukr. J. Phys.* **58**, 490 (2013).

23. I.M. Bolesta, I.N. Rovetskii, Z.M. Yaremko, I.D. Karbovnyk, S.R. Velgosh, M.V. Partyka, N.V. Gloskovskaya, and V.M. Lesivtsiv, *Ukr. J. Phys.* **60**, 1143 (2015).

24. I.M. Bolesta, I.N. Rovetskii, I.D. Karbovnyk, S.V. Rykhlyuk, M.V. Partyka, and N.V. Gloskovskaya, *J. Appl. Spectrosc.* **2**, 84 (2015).

25. I.B. Olenych, *Ukr. J. Phys. Opt.* **12**, 54 (2011).

26. A.I. Popov, E.A. Kotomin, and J. Maier, *Nucl. Instr. Meth. Phys. Res. B* **268**, 3084 (2010).

27. I. Bolesta, I. Rovetskii, I. Karbovnyk, and M. Partyka, *Techn. Phys. Lett.* **39**, 463 (2013).

28. G. Zimmerer, *Radiat. Meas.* **42**, 859 (2007).

29. P.V. Savchyn, V.V. Vistovskyy, A.S. Pushak, A.S. Voloshinovskii, A.V. Gektin, V. Pankratov, and A.I. Popov, *Nucl. Instrum. Meth. B* **274**, 78 (2012).

30. V. Pankratov, A.I. Popov, L. Shirmane, A. Kotlov, G.A. Bizarri, A. Burger, P. Bhattacharya, E. Tupitsyn, E. Rowe, V.M. Buliga, and R.T. Williams, *Radiat. Meas.* **56**, 13 (2013).

31. E. Shablonin, A.I. Popov, A. Lushchik, A. Kotlov, and S. Dolgov, *Physica B* **477**, 133 (2015).

32. A.V. Bystrova, Yu.D. Dekhtyar, A.I. Popov, J. Coutinho, and V.S. Bystrov, *Ferroelectrics* **475**, 135 (2015).

33. A. Kalinko, A. Kotlov, A. Kuzmin, V. Pankratov, A.I. Popov, and L. Shirmane, *Cent. Eur. J. Phys.* **9**, 432 (2011).

34. A.I. Popov, L. Shirmane, V. Pankratov, A. Lushchik, A. Kotlov, V.E. Serga, L.D. Kulikova, G. Chikvaidze, and J. Zimmermann, *Nuclear Instrum. Meth. Phys. Res. B* **310**, 23 (2013).

35. H. Matsumoto and H. Nakagawa, *J. Luminescence* **18-19**, 19 (1979).

36. S. Kawabata and H. Nakagawa, *J. Luminescence* **26**, 48 (2007).

37. K. Fukui, K. Asakura, K. Niimi, I. Ishizue, and H. Nakagawa. *J. Electron. Spectrosc. Rel. Phenom.* **101**, 299 (1999).